Self-assembled monolayers exposed by metastable argon and metastable helium for neutral atom lithography and atomic beam imaging

A. Bard
Atomic Physics Division, National Institute of Standards and Technology, Gaithersburg, Maryland 20899

K. K. Berggren
Department of Physics, Harvard University, Cambridge, Massachusetts 02138

J. L. Wilbur
Department of Chemistry, Harvard University, Cambridge, Massachusetts 02138

J. D. Gillaspy[a] and S. L. Rolston
Atomic Physics Division, National Institute of Standards and Technology, Gaithersburg, Maryland 20899

J. J. McClelland
Electron and Optical Physics Division, National Institute of Standards and Technology, Gaithersburg, Maryland 20899

W. D. Phillips
Atomic Physics Division, National Institute of Standards and Technology, Gaithersburg, Maryland 20899

M. Prentiss and G. M. Whitesides
Department of Chemistry, Harvard University, Cambridge, Massachusetts 02138

(Received 30 August 1996; accepted 7 July 1997)

We used a beam of noble gas atoms in a metastable excited state to expose a thin (1.5 nm) self-assembled monolayer resist applied over a gold-coated silicon wafer. We determined exposure damage as a function of dose of metastable atoms by processing the samples in a wet-chemical etch to remove the gold from unprotected regions and then measuring the reflectivity with a laser and observing the microstructure with an atomic force microscope. We found that the minimum dose required to damage the resist substantially was $1.7(3)\times10^{15}$ atoms/cm^2 for metastable helium, and $25(7)\times10^{15}$ atoms/cm^2 for metastable argon. © *1997 American Vacuum Society.*
[S0734-211X(97)03205-8]

I. INTRODUCTION

We recently demonstrated a new prototype method of microlithography[1] that uses a beam of neutral argon atoms in metastable excited states (Ar*) to expose an organic self-assembled monolayer (SAM). In these experiments, the substrate under the resist was a gold-coated silicon wafer. Samples were inserted into a beam of Ar* which had been patterned in the transverse direction using a physical mask. The exposure to metastables produced a pattern of damage in the SAM that was transferred by a wet-chemical etch onto the underlying gold. The patterned gold layer could then be used as a resist to form features in the underlying silicon substrate. Microstructures 5 μm wide with sharp (<100 nm wide) edges were generated using this technique.

In this article we investigate the dose-response behavior of the SAM resist to exposure by two metastable species with significantly different internal metastable excitation energies: Ar* (12 eV) and He* (21 eV). Metastable noble gas atomic beams are potentially suitable for lithography for several reasons: (1) they typically have a short de Broglie wavelength (<0.1 nm) which makes them relatively insensitive to diffraction, a limiting problem in lithography using ultraviolet light; (2) they can be patterned using physical masks as shown in Ref. 1 or by using atomic optics, e.g. focusing with laser light[2] or optical quenching by lasers;[3] (3) they are immediately quenched upon interaction with a surface, leaving a neutral inert gas atom in its ground state that can no longer damage the surface. Conventional lithographic agents (UV light, electrons) damage deep into a resist, an undesirable characteristic since scattering inside the resist can broaden a feature. Metastable atoms interact only with the outermost atomic layer of a surface and thus can provide concentrated damage to an ultrathin resist without penetrating into the underlying substrate. SAMs are a good thin resist for this application: they are only ~1.5 nm thick, and a number of studies have shown that they are useful for lithography when exposed to electron beams [conventional or via scanning tunneling microscopy (STM)], ions, or photons.[4–9] The SAMs are substantially damaged by low doses of metastable atoms, and hence allow patterns formed in a metastable atomic beam to be transferred into an underlying layer. The data in the present experiment determine the dose of metastable atoms needed to damage the SAM to a sufficient level to be useful as a prototype method of lithography. The method is still new and awaits considerable further development before its viability for production line lithography in an industrial setting can be determined.

An immediate potential application for a SAM is the detection of small (<100 nm) features in the center of mass

[a]Electronic mail: John.Gillaspy@NIST.gov

distributions of atoms. This is currently a challenging problem in atom optics. SAMs might be used as a high-resolution, two-dimensional detector for metastable atoms. Exposure of the SAM to a patterned beam of metastable atoms creates a pattern of damage in the SAM that can be transferred into an underlying gold substrate using a wet-chemical etch, and subsequently imaged using a variety of techniques such as atomic force microscopy (AFM) or scanning electron microscopy.

II. EXPERIMENTAL SETUP AND PROCEDURE

The experiment consists of four major steps: (1) preparation of a sample, (2) exposure of this sample to a beam of metastable atoms, (3) development of the sample by etching in a solution that contains ferricyanide, and (4) quantifying the amount of damage to the SAM by measuring the reflectivity of the remaining gold and by observing the gold microstructure with an AFM.

A. Sample preparation

Electron-beam evaporation was used to coat a polished Si<100>wafer with 2.5 nm of Ti (adhesion promoter) followed by 40 nm of Au (99.99%). The value of the gold thickness was chosen to assure a uniform coating, although smaller values, perhaps of a different material, could be used and would be warranted if this method is pushed to higher resolution in the future. The wafer was then fractured into rectangular samples of 1 cm×3 cm. The thickness of the gold was determined by protecting part of the sample with poly(methylmethacrylate) (PMMA), etching the unprotected gold using the PMMA as a resist, removing the PMMA, and measuring the height of the gold step edge with an AFM. The accuracy of the AFM measurement was verified by repeating the measurement with a second, independently calibrated, AFM. The two measurements agreed to better than the 11% AFM calibration specification.

SAMs were prepared on the gold surface by inserting the samples into a 0.202 g/l (~0.001 M) solution of dodecanethiol $CH_3(CH_2)_{11}SH$ in ethanol for at least 24 hours. All glassware used for this step of the experiment was "Piranha" cleaned.[10] Dodecanethiol was obtained from a commercial source and was purified by distillation prior to use. Samples were removed from this solution, rinsed by dipping into absolute ethanol, and inserted immediately (<2 min) into the loading chamber of the atomic beam apparatus.

B. Exposure to metastables

Figure 1 shows a schematic of the experimental atomic beam apparatus. The metastable atoms were produced by a low pressure gas discharge similar to the one described in Ref. 11. The discharge consisted of a sharpened tungsten cathode in the center of a quartz tube with a nozzle of approximately 120 μm diameter at one end. The working pressure inside the quartz tube was maintained at 1 kPa for argon and 4 kPa for helium. A skimmer, located 7 mm from the nozzle and having a 1-mm-diam aperture, served as the anode of the discharge. The space between the quartz nozzle

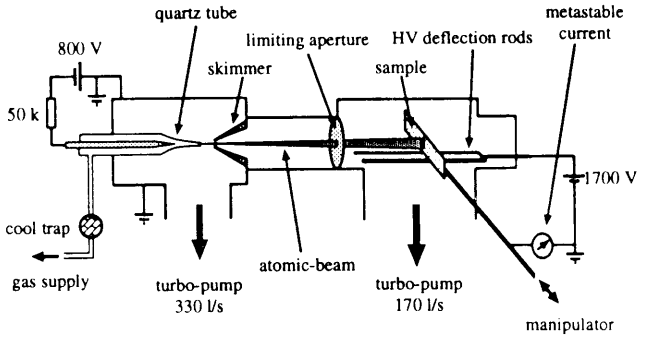

FIG. 1. Experimental setup of the metastable beam apparatus.

and the skimmer was differentially pumped by a turbomolecular pump to a pressure between 10^{-3} and 10^{-2} Pa (10^{-5}–10^{-4} Torr), depending on the pressure in the quartz tube. The beam emitted through the skimmer was roughly collimated by a final aperture to 39(2) mrad.[12] The resulting beam diameter was 7.5 mm in the observation chamber, a distance of 20(1) cm away from the discharge. The atomic beam apparatus also had a separately pumped loading chamber for sample insertion and manipulation.

The flux of metastable atoms was determined by measuring the current produced in a detector plate positioned at the end of the atomic beam apparatus. This current is due to the emission of secondary electrons from the plate upon metastable impact.[13,14] We used graphite-coated stainless-steel plates for measurements of the flux of Ar* and stainless-steel plates for He*. The accuracy of this method is discussed in detail below. Because the sample was mounted between the skimmer and the detector it was not possible to measure the current at the detector during exposure of the samples. To determine changes in the flux while samples were being exposed, however, we monitored the current induced on the sample itself.

Discharges similar to the one used are known to produce electrons, ions, fast neutral atoms, and vacuum ultraviolet (VUV) photons as well as metastable atoms. The charged particles were deflected away from the sample using aluminum deflection rods at a positive high voltage of 1700 V. By quenching the dominant portion of the Ar* flux with a titanium-sapphire laser at 764 nm, we have previously demonstrated[7] that the primary source of exposure in these experiments was due to the metastable atoms and not to any other species in the discharge (charged or uncharged). In the present work we have added a second laser at 795.6 nm to quench the remaining fraction of the Ar* flux (the Ar^* P component), and find a residual detector current of only 6% of the full value. We suppose that this residual current may be due to fast neutrals and/or VUV photons. This double-laser measurement allows us to determine the Ar^* $^3P_1$ component of our beam to be 17% and the Ar^* $^3P_2$ component to be 83%, in good agreement with the expected statistical mixture of 5:1. Since laser quenching was not possible in the case of He* we filled the observation chamber with 0.1 Pa of either argon or nitrogen to remove He* by collisional quenching. We verified that the measured detector current

dropped to about 8% of it's original value after introducing the quench gas. We suppose that the measured current was due to fast neutrals, helium VUV photons, or perhaps ions of argon or nitrogen produced by helium VUV photons. In any case, samples exposed during the presence of either a quench laser (in the case of argon) or a quench gas (in the case of helium) showed no measurable damage after etching. This shows clearly that the beam component that is responsible for the residual signal does not damage the SAM sufficiently during our exposure times to be observed outside of the present level of experimental uncertainty. We therefore neglect the residual beam component for this study, but note that it may become important for any future work which is carried out at doses very high compared to those used here.

The pressure in the observation chamber during the measurement was 8×10^{-4} Pa when working with argon and 7×10^{-3} Pa when working with helium. The pressure was due mainly to the presence of gas from the discharge since the pressure in the observation chamber dropped to less than 10^{-6} Pa when the gas supply was switched off. We used a dry-ice cold trap on the gas supply tube to remove any contaminants that may have been present. We used a residual gas analyzer to verify that, on a partial pressure level of 10^{-8} Pa, there were no hydrocarbon contaminants smaller than 200 amu present in the observation chamber.

The samples were mounted on a holder at the end of a 30-cm-long vacuum manipulator and brought into the observation chamber through the loading chamber. The pressure in the loading chamber was reduced from atmospheric pressure to ~0.5 Pa over a 10 min period to avoid possible contamination or damage to the SAM from rapid gas flow. A small turbopump was then used to lower the pressure to a presumed value of $\sim10^{-4}$ Pa before the loading chamber was opened to the observation chamber. The operation of ion gauges was found to damage SAMs, so the pressure was only measured in control runs where no SAMs were actually used. We exposed samples for times that ranged from several minutes to several hours, depending on the extent of damage that was desired.

C. Etching

After exposure, the sample was removed from the vacuum chamber and immediately immersed in an etching solution to remove the gold from regions where the SAM was sufficiently damaged by the metastable atoms to allow penetration of the etchant. The etching solution consisted of: 56.0 g/l (1 M) potassium hydroxide (KOH), 19.0 g/l (0.1 M) potassium thiosulfate ($K_2S_2O_3$), 11.8 g/l (0.01 M) potassium ferricyanide ($K_3Fe(CN)_6$), and 1.22 g/l (0.001 M) potassium ferrocyanide ($K_4Fe(CN)_6$). Prior to use, the etching solution was filtered with a 10–20 μm sintered-glass filter to remove solid particles. The etching was performed in the particular geometrical configuration (Figure 2) that was found to give the best reproducibility. The samples were etched for 20 min, removed from the etching solution, washed with distilled water and dried with a stream of dry, filtered nitrogen gas. The 20 min etch time was chosen to yield good contrast, based on previous experience with samples heavily exposed with metastable argon studied as a function of etch time.[1]

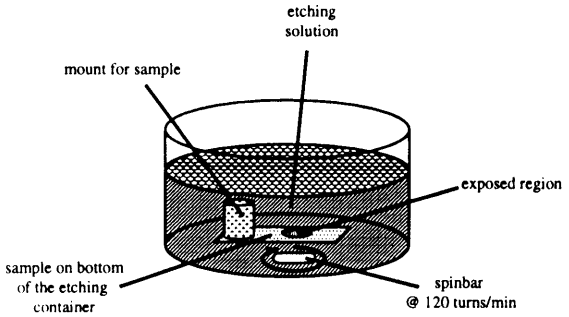

FIG. 2. Configuration for etching the samples which provided the best reproducibility.

D. Reflectivity measurements

To determine the amount of gold removed during the etching process, we used the apparatus shown in Figure 3 to measure the reflectivity of light from a HeNe laser (632.8 nm) at normal incidence. In this measurement, we took six one-dimensional scans of the reflectivity, each separated by a distance of 1 mm in the lateral direction. The laser beam was sufficiently focused that we could image a test grid which had a 23 μm bar width; the calculated spot size was 15 μm on the surface of the sample. In order to cover the exposed region (7.5 mm diameter) and the adjacent unexposed regions, we used a typical scan length of 25 mm with 500 data points. We checked the linearity of the intensity response function of the photodiode to better than 1%. By subsequently studying the surface structure with an atomic force microscope we were able to make estimates of the amount of gold removed as a function of reflectivity, and found that under our conditions reflectivity is a good measure of the amount of gold remaining on the sample.

III. RESULTS AND DISCUSSION

Figure 4 shows an atomic force micrograph of a sample that was exposed with argon metastable atoms and etched as described above. The image shows the formation of pits with a lateral size on the order of 50 nm. The maximum height of the surface features is smaller than the original gold thick-

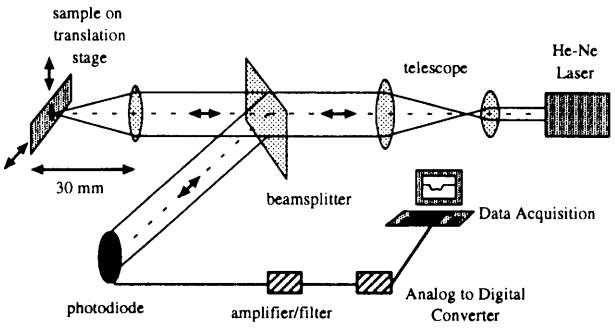

FIG. 3. Experimental setup used to determine the reflectivity.

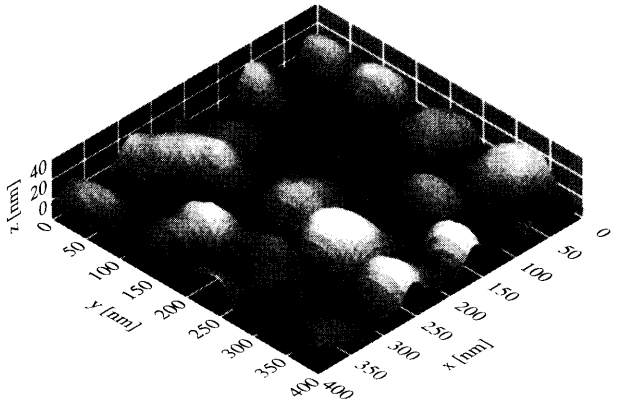

FIG. 4. Atomic force micrograph of a sample with 52% reflectivity after exposure with metastable argon and etching as described in the text.

ness of 40 nm. Because the surface structure (in all three dimensions) is small compared to the wavelength of red light, the reflectivity measurement at 633 nm effectively averages over the pits and yields a result nominally equivalent to a uniform film composed of the same amount of gold. The reflectivity of 52% measured on this sample corresponds to a gold thickness of 16 nm. This inferred thickness is approximately equal to the mean height of the residual gold measured with the AFM in this case.

Figures 5 and 6 show the reflectivity of the sample versus the dose of metastable argon (Ar*) and metastable helium (He*), respectively. To obtain the reflectivity for each dose of metastable atoms, we averaged the results for all samples that received the same dose. We also performed experiments in which we exposed several areas on one sample; data from these experiments showed the same trend as that observed in larger data sets composed of exposures made on different samples. In averaging the data, we treated each of the exposed areas as an independent exposure. The 12 points shown in Figures 5 and 6 for doses other than zero are averages derived from a total of 26 independent exposures. The values for each dose level are generally averages of two to six points, though some are single measurements (Ar* doses 14, 16 and 28×10^{15} atoms/cm^2, and He* doses 0.13, 1.3 and 5.2×10^{15} atoms/cm^2). Also shown in the figures (horizontal dashed lines) are the measured values of reflectivity for bare silicon and for unprocessed, gold-coated silicon.

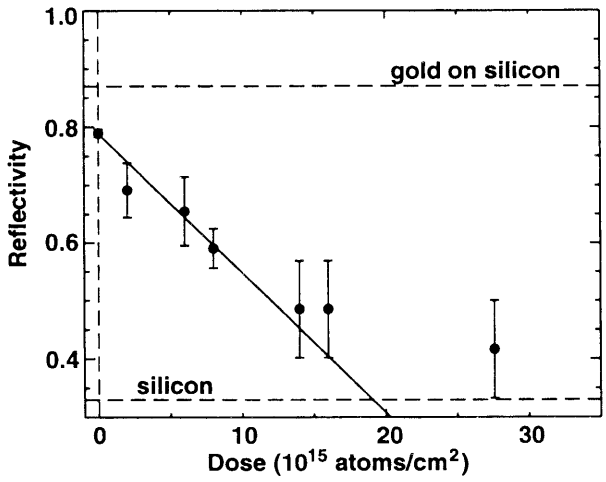

FIG. 5. Reflectivity of samples at 632 nm after receiving a certain total dose of Ar*. The surface density of the SAM molecules is 4.6×10^{14} molecules cm^{-2}.

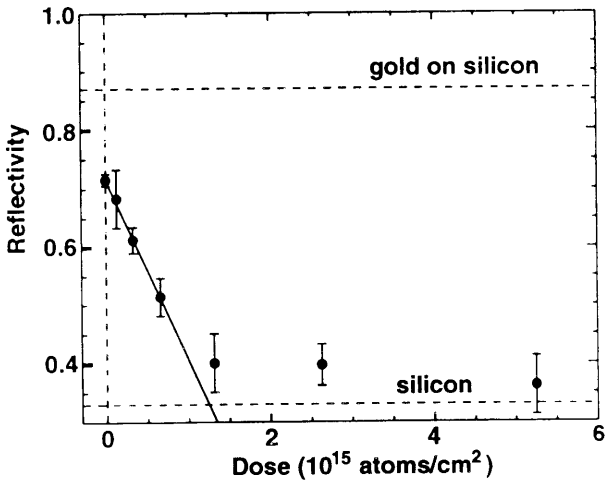

FIG. 6. Reflectivity of samples at 632 nm after receiving a certain total dose of He*. The surface density of the SAM molecules is 4.6×10^{14} molecules cm^{-2}.

The data show that, for both Ar* and He*, the exposure saturates above a certain dose of metastable atoms. Well below the saturation limit, the reflectivity decreases linearly with increasing dose of metastables (within experimental uncertainty). We determined the slope of this decrease by performing a weighted least-squares linear fit to only the low-dose, unsaturated measurements (below 15×10^{15} atoms cm^{-2} for Ar*, or 1×10^{15} atoms/cm^2 for He*). The resulting lines are shown in Figures 5 and 6. The weights chosen for the fit were taken from the uncertainties, which are displayed as error bars in the plots. For dose values with three or more measurements, the uncertainties are the standard deviation of the measurements, divided by the square root of the number of measurements. For doses with two or less exposures, an assumption was made that the variance would be similar to that of the doses with more measurements, and the average variance of all doses with three or more exposures was used to estimate the standard deviation. This is divided by the square root of the number of measurements (2 or 1) to give the uncertainties for the points with few measurements.

The reflectivity value corresponding to a dose of zero was the average of the reflectivities of the unexposed regions to the left and right of the exposed regions of all samples studied with a given gas. There were 15 such measurements for Ar* and 20 for He*. We used the reflectivity of unexposed regions of gold (that were etched along with the exposed region) for the zero-dose point rather than the reflectivity of untreated gold to account for possible damage by processing that may have affected the whole sample. We found the reflectivity of untreated gold to be 11% higher than that of the

background regions in the case of Ar* and 21% in the case of He*. This effect may have been due to partial breakdown of the unexposed SAM during processing, but we do not have an adequate explanation for the difference between the cases of He* and Ar*. The fact that the measured reflectivity at high metastable atom dose is noticeably above the pure silicon value may be due to the presence of a residual Ti layer. The full initial 2.5 nm thickness of Ti is calculated to contribute an additional 5% to the reflectivity. The Ti underlayer is expected to be resistant to the 20 min etch used in this work.

To calibrate the flux, we used published values of the efficiency (ε) for the ejection of electrons by a metastable atom. For He*, Dunning *et al.*[13] found $\varepsilon_{st,He,3}=0.69(10)$ and $\varepsilon_{st,He,1}=0.53(8)$ for the impact of metastable helium triplets and singlets, respectively, on a stainless-steel plate. Taking into account the flux ratio of both components, we obtain $\varepsilon_{rm\ He,st,mix}=0.64(10)$ for the mixture (singlet/triplet=0.37)[15] in our source.

For all noble gases other than helium and neon, the value of ε depends strongly on the preparation of the detector surface.[13,14] This introduces a large uncertainty in the value of ε_{Ar}, which dominates our uncertainty for the measurement of flux. Schohl *et al.*[14] found $\varepsilon_{Ar}=0.20$ for Ar* $^3P_2$ on a freshly prepared surface of colloidal graphite on polished stainless steel. This was found to be the most reproducible of all the surfaces they studied. The conditions in our system — including the base pressure in the observation chamber — are very similar to the conditions in the apparatus of Schohl *et al.*, and we implemented the detector surface preparation procedure used by those authors.[14] In other measurements, Schohl *et al.*[14] showed that the difference in electron ejection efficiencies on graphite for excited atomic levels that differ by 1.5 eV is 15%. Considering the small energy difference (0.08 eV) between Ar* $^3P_0$ and Ar* $^3P_2$, and the small (20%) fraction of Ar* $^3P_0$, we can safely use the value $\varepsilon_{Ar,graphite,mix}=0.20(5)$ as the detection efficiency for the mixture of Ar* $^3P_0$ states and Ar* $^3P_2$ states in our atomic beam. (We also did experiments using a bare stainless-steel plate as a detector, and then calibrated the plate by comparison with the graphite surface to obtain $\varepsilon_{Ar,steel,mix}=0.15$, well inside the range of $\varepsilon_{Ar,steel,mix}=0.04$–$0.22$ that was found by Schohl *et al.*[14] for bare stainless steel). The measured detector currents and the related fluxes for helium and argon are given in Table I.

The ratio of the slopes of the linear part of the reflectivity curves for exposure with Ar* and He* (Figures 5 and 6) is $s_{He}/s_{Ar}=15(5)$ (the statistical contribution arising from the weighted least-squares fit contributes 2 to the overall uncertainty quoted). The damage was clearly not linearly proportional to internal metastable energy since the ratio of the excitation energies is only $E_{He}/E_{Ar}=1.7$. This is consistent with the work of Borst,[16] who found a highly nonlinear functional relationship of the electron emission coefficient ε versus the excitation energy E for metastable atoms on beryllium-copper oxide. However, the SAM damage ratio, s_{He}/s_{Ar} is also significantly greater than the ratio $\varepsilon_{He}/\varepsilon_{Ar}$ of

TABLE I. Metastable-detector current and resulting metastable flux for argon and helium.

Atom	Current (nA/44.2 mm^2)	ε	Flux (10^{12} s^{-1} cm^{-2})
Argon	23.5	0.20	1.7
Helium	99.1	0.64	2.2

detector coefficients. This shows that helium is much more efficient for this type of lithography than argon, and underscores the need for better understanding of the underlying mechanism for the damage of SAM resists by metastable atoms.

In order to have an indicator of the absolute dose required to expose a SAM resist, we define an exposure dose D_o as the dose required to damage the SAM resist sufficiently that the underlying gold is unprotected and the postetch reflectivity is into the saturated (bare silicon) regime in Figures 5 and 6. Specifically, D_o is the reciprocal of the slope of the reflectivity-dose curve (s^{-1}), multiplied by R, the reflectivity change corresponding to complete removal of the gold (R is taken to be 0.54 here). For Ar*, $D_o=25(7)\times10^{15}$ atoms/cm^2, while for He*, $D_o=1.7(3)\times10^{15}$ atoms/cm^2.

Assuming that the secondary electrons that are produced by the impact of metastable atoms are at least in part responsible for the damaging of the SAM, one may compare the charge deposited to the dose used when exposing SAMs to an electron beam or by using a scanning tunneling microscope (STM). In our experiment, if we assume one electron per metastable atom, the typical charge for the SAM exposure is roughly 4×10^{-3} C/cm^2 for Ar* and 3×10^{-4} C/cm^2 for He*. Baer *et al.*[8] find in their electron-beam experiments a dose of 7.5×10^{-3} C/cm^2 for the exposure of monolayers formed from octadecyltrichlorosilane ($Cl_3Si(CH_2)_{17}CH_3$) on Si oxide. Taking into account that we used shorter SAMs with only 12 C atoms per molecule, both methods are roughly of the same sensitivity. In a typical STM experiment Perkins *et al.*[9] use doses of 2.2 C/cm^2 to expose monolayers formed from (aminoethylaminomethyl)phenethyltrimethoxysilane [$(CH_3O)_3Si$-$(CH_2)_2$-C_6H_4-CH_2-NH-$(CH_2)_2$-NH_2)]. Though this is not the exposure limit (the dose may have been far above the minimum dose threshold), it shows that this method significantly differs from the others with regard to the deposited charge.

A potentially important source of uncertainty in the experiment was in the calibration of the reflectivity measurements. The raw reflectivity data (photodiode current) was converted into absolute reflectivity by dividing by the current observed for a calibration sample of bare silicon and multiplying by the calibration factor 33(1)%. The calibration factor was obtained by measuring both the incident and reflected power from a sample of our bare silicon. This calibration was confirmed by measurements in which reflected power for our bare silicon was compared to that for a high-reflectivity dielectric mirror (the two methods agreed to within 1%). Furthermore, our measured bare-silicon reflectivity is in reasonable agreement with the value predicted at

632 nm (35.2%) by using the equations and constants given in Ref. 17. By mounting the same sample more than once it has been shown that random uncertainties in the acquisition of the reflection data, including both random detector noise and uncertainties in the angular position of the sample during the reflection measurement, are lower than 5%. This source of uncertainty is therefore only minor.

Large inhomogeneities in the etched surface were frequently observed. These were in the form of streaks with a width of a few tenths of a mm and irregular larger areas (~ 1 cm^2) where more gold had been removed. After averaging the inhomogeneities, remaining sample-to-sample scatter ($\approx 7\%$) in reflectance data was observed when multiple independent exposures were taken at the same dose. These inhomogeneities, and the resulting uncertainty in the reflectivity data, were largely due to irreproducibilities in etching. Several tests were performed in order to establish a reproducible process for etching. Inhomogeneities were sometimes also observed on control samples that were etched without exposure. The etching configuration shown in Figure 2 was found to give the highest overall reproducibility of the averaged reflectivity data. We do not believe that the inhomogeneities are a fundamental aspect of the process, and are confident that future refinements of the technique will be devised to overcome them. Furthermore, we note that in a practical setting, resist exposure would typically take place significantly beyond the minimum dose threshold in order to wash out any exposure inhomogeneity.

IV. CONCLUSION

We have investigated the effect of metastable atom bombardment on the ability of a self-assembled monolayer to function as a protective resist against wet-chemical etching. The damage to the resist was quantified by using the resist to protect a gold-coated silicon wafer, chemically etching the coated wafer, and then using a laser to measure the reflectivity of the remaining gold and an AFM to examine the microstructure of the surface. The amount of gold remaining after etching was found to decrease approximately linearly towards zero, saturating above an exposure dose $D_o = 25(7) \times 10^{15}$ atoms/cm^2 for Ar* and $D_o = 1.7(3) \times 10^{15}$ atoms/cm^2 for He*. Two applications for which these results may be useful are (1) the use of SAMs as a resist for neutral atom lithography, and (2) the use of SAMs as a two-dimensional detector for metastable atoms.

We found that the saturating dose was not simply proportional to the energy of the metastable states since the damage per helium atom is 15 times higher than the damage per argon atom while the energy of the metastable states differs only by a factor of roughly 2. This result suggests that helium is better suited for lithographic applications where the rate of the process is an important parameter.

Note added in proof: subsequent to completion of this work, a similar study was reported by S. Nowak, T. Pfau, and J. Mlynek, Appl. Phys. B **63**, 203 (1996).

ACKNOWLEDGMENTS

The authors thank D. C. Parks for the AFM imaging. A.B. acknowledges financial support from the Alexander von Humboldt Foundation and NIST. J.L.W. gratefully acknowledges a postdoctoral fellowship from the NIH (Grant No. 1-F32 GM16511-01). This work was partially supported by NSF Grant No. PHY 9312572. This work also made use of the MRSEC Shared Facilities supported by the NSF under Award No. DMR-9499396.

[1] K. K. Berggren, A. Bard, J. L. Wilbur, J. D. Gillaspy, A. G. Helg, J. J. McClelland, S. L. Rolston, W. D. Phillips, M. Prentiss, and G. M. Whitesides, Science **269**, 1255 (1995).
[2] G. I. Timp, R. L. Behrenger, D. M. Tennant, J. E. Cunningham, M. Prentiss, and K. K. Berggren, Phys. Rev. Lett. **69**, 1636 (1992); J. J. McClelland, R. E. Scholten, E. C. Palm, and R. J. Celotta, Science **262**, 877 (1993); K. K. Berggren, M. Prentiss, G. Timp, and R. E. Behringer, J. Opt. Soc. Am. B **11**, 1166 (1994).
[3] A. P. Chu, K. K. Berggren, K. S. Johnson, and M. G. Prentiss (in press).
[4] M. J. Lercel, G. F. Redinbo, F. D. Pardo, M. Rooks, R. C. Tiberio, P. Simpson, H. G. Craighead, C. W. Sheen, A. N. Parikh, and D. L. Allara, J. Vac. Sci. Technol. B **12**, 3663 (1994).
[5] J. M. Calvert, T. S. Koloski, W. J. Dressick, C. S. Dulcey, M. C. Peckerar, F. Cerrina, J. W. Taylor, D. Suh, O. R. Wood II, A. A. MacDowell, and R. D'Souza, Opt. Eng. (Bellingham) **32**, 2437 (1993).
[6] C. S. Dulcey, T. S. Koloski, W. J. Dresick, M. S. Chen, J. H. Georger, and J. M. Calvert, Proc. SPIE **1925**, 657 (1993).
[7] E. T. Ada, L. Hanley, S. Etchin, J. Melngailis, W. J. Dressick, M.-S. Chen, and J. M. Calvert, J. Vac. Sci. Technol. B **13**, 2189 (1995).
[8] D. R. Baer, M. H. Engelhardt, D. W. Shulte, D. E. Guenther, and Li-Q. Wang, J. Vac. Sci. Technol. A **12**, 2478 (1994).
[9] F. K. Perkins, E. A. Dobisz, S. L. Brandow, T. S. Koloski, J. M. Calvert, K. W. Rhee, J. E. Kosakowski, and C. R. K. Marrian, J. Vac. Sci. Technol. B **12**, 3725 (1994).
[10] **Warning:** 30% H_2O_2 and 70% H_2SO_4 Pirahna solution is extremely caustic. Use only with extreme caution.
[11] D. W. Fahey, W. F. Parks, and L. D. Schearer, J. Phys. E **13**, 381 (1980).
[12] The uncertainty limits here and throughout this article are one combined standard uncertainty unless otherwise stated.
[13] F. B. Dunning, R. D. Rundel, and R. F. Stebbings, Rev. Sci. Instrum. **46**, 697 (1975).
[14] S. Schohl, D. Klar, T. Kraft, H. A. J. Meijer, M.-W. Ruf, U. Schmitz, S. J. Smith, and H. Hotop, Z. Phys. D **21**, 25 (1991); S. Schohl, H. A. J. Meijer, M. W. Ruf, and H. Hotop, Meas. Sci. Technol. **3**, 544 (1992).
[15] Craig J. Sansonetti (unpublished results).
[16] W. L. Borst, Rev. Sci. Instrum. **42**, 1543 (1971).
[17] *American Institute of Physics Handbook* 3rd ed., edited by D. E. Gray (McGraw-Hill, New York, 1972).